JOURNAL OF MATERIALS SCIENCE **40** (2005) 2519–2523

Pressure infiltration of Al-Si alloys into compacts made of carbon particles

A. RODRÍGUEZ*, S. A. SÁNCHEZ, J. NARCISO
Departamento de Química Inorgánica, Universidad de Alicante, Apartado 99, E-03080, Alicante, Spain
E-mail: Alejandro.Rodriguez@ua.es

E. LOUIS
Departamento de Física Aplicada, Universidad de Alicante, Apartado 99, E-03080, Alicante, Spain; Unidad Asociada del Consejo Superior de Investigaciones Científicas, Universidad de Alicante, Apartado 99, E-03080, Alicante, Spain

F. RODRÍGUEZ-REINOSO
Departamento de Química Inorgánica, Universidad de Alicante, Apartado 99, E-03080, Alicante, Spain

In this work several aspects of pressure infiltration of Al and Al-12wt%Si eutectic alloy into preforms of packed carbon particulates have been investigated. Compacts were prepared from particles of average diameter 13.5, 26 and 61.6 μm. While infiltration with pure Al at 750°C was very poor due to the extensive reaction between C and Al, the substantial lowering of the infiltration temperature that allows the use of Al-Si eutectic alloy, greatly improved infiltration performance. Results for the threshold pressure and infiltration kinetics are discussed in the light of previously published results for different systems. The effect of Ti addition has also been investigated.

1. Introduction

One of the material families that is being considered by the automotive industry as a replacement for standard materials, is that of carbon preforms infiltrated with light metals, mostly aluminium [1–3]. These materials are expected to exhibit the high strength, lightweight, and good thermal properties required in automotive components. Pressure infiltration is probably the fabrication method best suited to produce the variety of the complex shapes for engine components. Two important limitations to the fabrication of Al-C composites by liquid-phase routes are: (i) the gasification of carbon, that initiates around the melting temperature of pure aluminium, and (ii) the reaction between Al and carbon to form aluminium carbide, an unstable compound with very poor properties. Si addition is highly beneficial in this system because it permits a substantial drop in the fabrication temperature, thus reducing the reaction between aluminium and carbon.

It is generally accepted that wettability at the Al/C interface and reactivity between the two materials should greatly influence the final properties of the composite. Wettability is usually evaluated by measuring the contact angle at the liquid/solid interface [4, 5]. Unfortunately, contact angle measurements in the Al/C system are scarce. Recent results reported by Landry *et al.* [6] indicate that Si addition decreases the contact angle at the Al/C interface. Coating of the graphite reinforcement prior to metal infiltration is also being explored to improve the compatibility between the two materials.

In this work we present experimental data for pressure infiltration of liquid aluminium, Al-12Si and Al-12Si-1Ti alloys into packed samples of graphite particles with average diameters in the range 14–62 μm with a volume fraction slightly above 0.5. Infiltration was carried out at temperatures in the range 913–1013 K. The intrinsic permeability of the carbon particulate preforms was evaluated from infiltration with polyethyleneglycol (PEG). Experimental results indicate that infiltration kinetics followed Darcy law. The results presented here indicate that the reaction at the graphite/aluminium interface plays an essential role in the performance of the infiltration kinetics and very likely in the final properties of the composite.

2. Materials and experimental procedures

High purity aluminium (99.98%), and Al-Si-Ti alloys of composition reported in Table I, were used in the infiltration experiments of compacted graphite particles (of 13.5, 26 and 61.6 μm average diameter). The main characteristics of the graphite particulate are given in

*Author to whom all correspondence should be addressed.

TABLE I Chemical compositions of the Al-Si alloys used in this work

Alloy	Si	Ti	Cu	Fe	Ni	Others
A1	12	–	0.04	0.1	–	0.09
A2	11.6	–	1	0.7	0.06	0.5
A3	12	0.5	0.04	0.1	–	0.15
A4	12	1	0.04	0.1	–	0.1
A5	12	1.5	0.04	0.1	–	0.05

TABLE II Average diameter D (in μm) of graphite particulate used in this work

Particulate	D	Span	S
Graphite	13.5	1.38	7.71
	26	0.98	3.61
	61.6	0.94	0.95

The span of the particle size distribution is defined as $[D(90) - D(10)]/D(50)$. $D(x)$ is the diameter (also in μm) below which x% of the particles are found. The specific surface area of the particles S (m^2/g), as measured by means of nitrogen adsorption technique, is also given.

Table II. Graphite particles were chosen because the overall objective of this long-term research is infiltration of graphite preforms.

The particulates were packed into quartz tubes of 4.5-mm ID X 20-cm length by alternating vibrations and strokes of a rod. A rubber disc attached to the piston considerably reduced breaking of the brittle graphite particles. At each packing step, approximately 0.033 g of particulate were added and subjected to 2 seconds of vibrations and 20 strokes of a 35 g rod dropped from a height of 10 cm. The process was repeated until the compact reached a height of ≈3.5 cm. In order to determine the particle volume fraction V_p, the quartz tube was weighed before and after the powder was packed inside it, and its diameter measured at five points along its perimeter. Then a measure of the length of the packed powder allowed to obtain V_p. The helium density of the graphite particulates used in this determination was 2.16 $g \cdot cm^{-3}$. As shown in Table III, the resultant volume fraction V_p is very similar for the three particle sizes used here. The quartz tube containing the packed powder was attached at the top of the pressure chamber and immersed into the liquid metal.

The alloys were melted in alumina crucibles of 45-mm ID X 72-mm height. The infiltration system used in this work is described elsewhere [7, 8]. Infiltration was carried out at temperatures in the range 913–1013 K. Higher temperatures induced extensive gasification of graphite particles. Before each experiment, the metal was degassed by bubbling argon gas and its surface cleaned. As no inert atmosphere was introduced into the packed powder, it is expected that a thin oxide layer will cover the surface of the alloys throughout the whole infiltration process. The compacts were preheated for 80 seconds by holding the quartz tube just above the melt. Longer preheating times may lead to some depacking produced by graphite combustion. The chamber was closed and pressure was applied with nitrogen gas at a rate of 50 to 60 kPa $\cdot s^{-1}$ up to the chosen pressure. After a fixed period of time, the chamber was vented at a rate of 30 to 70 kPa s^{-1}. The sample was taken out of the melt and air-cooled and it was sectioned and the infiltration height measured with a precision gauge.

Polyethyleneglycol-200 of 99% purity, supplied by Panreac, was also infiltrated into the C compacts at room temperature, to evaluate their intrinsic permeability. The infiltration height was measured at different times after infiltration was initiated. Top or bottom infiltration gave very similar results, indicating that gravity plays no role in the process which turns out to be essentially determined by wetting at the graphite/PEG interface. The contact angle at the graphite/PEG interface was measured following the procedures described in [9], the result being $\theta = 5^\circ$.

TABLE III Results of the infiltration experiments at different temperatures for the aluminium alloys and the graphite particulate of Tables I and II respectively

Alloy	T (K)	γ_{lv}	D (μm)	V_p	P_0
A1	913	855	13.5	0.531	1439
			26	0.527	622
			61.6	0.523	283
	963		26	0.524	627
	1013		26	0.528	610
A2	913	830	13.5	0.534	1440
			26	0.521	603
			61.6	0.526	275
A4	913	856	26	0.529	631
	1013		26	0.528	614
			61.6	0.517	273
A3	913	858	26	0.53	626
A5	913	855	26	0.527	631

P_o is the threshold pressure for infiltration in kPa, V_p is the volume fraction of the particulate and γ_{lv} (in $mN \cdot m^{-1}$) is the surface tension of the metal [13–15].

3. Results and discussion

As shown in Fig. 1 the experimental results for infiltration of the alloy A2 of Table I into a preform made of the smallest particle used here follows Darcy law,

$$h^2 = \frac{2kt}{\mu(1 - V_p)}(P - P_0) \qquad (1)$$

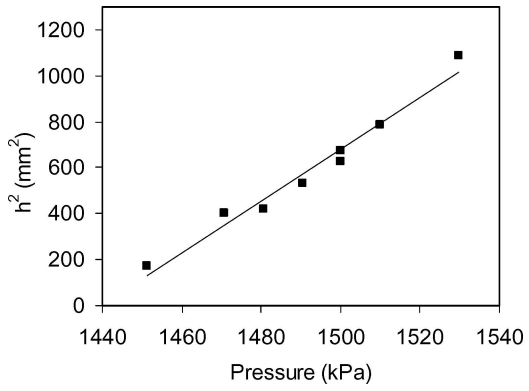

Figure 1 Square of the infiltrated height h^2 versus the applied pressure P for compacts of the 13.5 μm graphite particle of Table II infiltrated with alloy A2 of Table I.

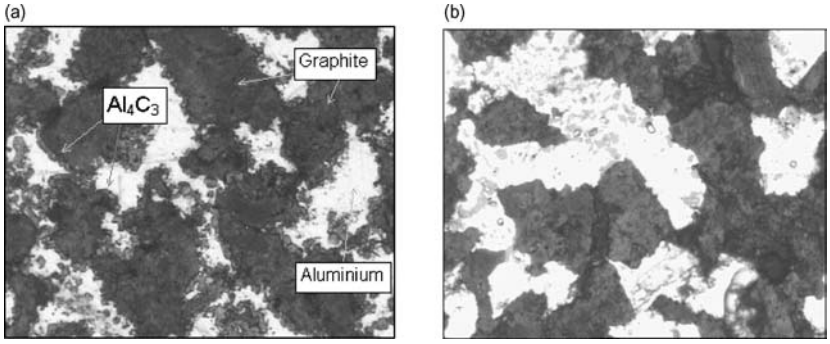

Figure 2 Optical micrographs of composites fabricated by infiltration of compacts of 26 μm graphite particles with: (a) pure aluminium and (b) A2 alloy of Table I.

where k is the permeability of the compact, V_p the particle volume fraction and μ the viscosity of the alloy. The straight line in Fig. 1 allows to derive the threshold pressure for infiltration P_0 and the permeability of the compact. Similar infiltration experiments with pure aluminium did not yield reasonable results. The optical micrograph of Fig. 2a clearly illustrates the very extensive reaction that occurs when C compacts are infiltrated with pure aluminium. The reaction is sharply reduced when pure Al is replaced by Al-Si alloys (Fig. 2b). It is worth noting that due to the relatively low infiltration temperatures and short infiltration times, no gasification of graphite particles was observed.

3.1. Threshold pressure for infiltration

The threshold pressure for infiltration P_o (also called capillary pressure) in Equation 1 is related to the contact angle θ and the particle average particle diameter D through the so-called capillary law or Laplace equation [10]

$$P_0 = -6\lambda\gamma_{lv}\cos\theta\frac{V_p}{(1-V_p)D} \qquad (2)$$

where γ_{lv} is the liquid-vapor surface tension and λ a factor which depends on the geometry of the particles.

Experimental results for the threshold pressure for infiltration of Al-Si alloys into graphite compacts are reported in Table III. Plots for the square of the infiltrated height versus applied pressure are illustrated in Fig. 3. Threshold pressure results were very similar for all the alloys of Table I. Ti addition had no significant effect. This result does not contradict the observed decrease in contact angle at the Al/C interface promoted by Ti addition, as the effect was only significant above 1300 K [11]. As shown in Fig. 4, the change in the threshold pressure with particle diameter follows the $1/D$ law predicted by the Laplace equation for all the alloys investigated here. The results plotted in this figure were obtained by inserting in Equation 2 the surface tension of each alloy and the contact angle (135°) at the graphite/Al-12Si interface [6] (no significant changes in contact angle are expected to occur upon Si or Ti additions at 913 K at short times). A fitting of these results by means of a straight line gives $\lambda = 4.56$.

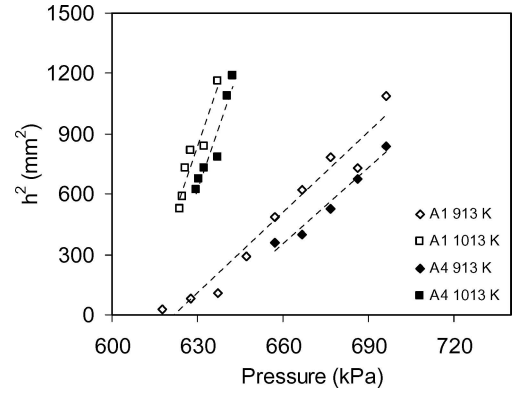

Figure 3 Plot of h^2 as a function of applied pressure P for packed 26 μm graphite particulate infiltrated with A1 and A4 alloys at 913 K and 1013 K.

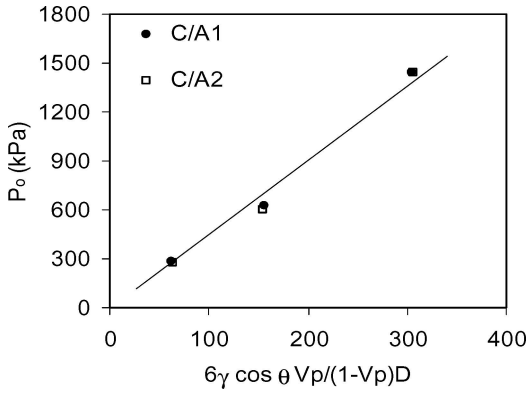

Figure 4 Threshold pressure P_o for the graphite particulate infiltrated with A1 and A2 versus $6\lambda\gamma_{lv}\cos\theta V_p/(1-V_p)$ D.

3.2. Darcy law: Permeability of the compacts

The results shown in Fig. 3 clearly indicate that the higher the temperature the faster the infiltration rate. This is in line with the decrease in the viscosity of liquid metals as the temperature is raised. However, the results indicate that the slope of the straight lines in Fig. 3 change with temperature at a pace greater than the viscosity of aluminium-silicon alloy [12]. This can be explained due to the increase of saturation at high temperature. Fig. 5 shows the square of the infiltrated height versus the pressure drop $P - P_0$ obtained from infiltrations of alloy A1 of Table I into compacts made of the three carbon particles of Table II. The results

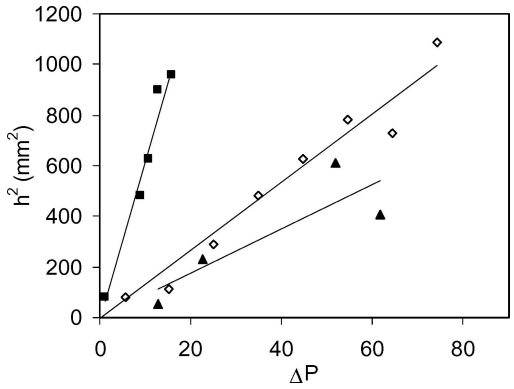

Figure 5 Square of the infiltrated height h^2 versus ΔP for (▲)13.5, (◇) 26 and (■) 61.6 μm graphite particulate (see Table II) compacts infiltrated with alloy A1 of Table I.

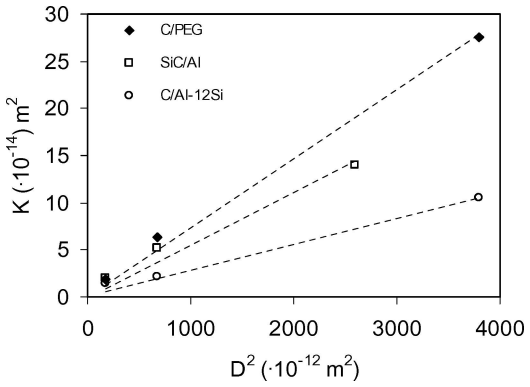

Figure 6 Intrinsic permeability of particle compacts versus the square of the particle diameter for the following systems: C/PEG, C/A1 alloy and SiC/Al (see text).

follow the expected trend: monotonic increase of the infiltration rate with particle size (see below).

In order to throw light on the above results the intrinsic permeability of the compacts was evaluated through infiltrations of PEG. As PEG wets carbon the experiments were carried out with no external pressure and varying the infiltration time. Under these conditions the square of the infiltrated height is proportional to the capillary pressure. Then, to derive the intrinsic permeability, data related to the compact (particle diameter, geometric factor and volume fraction), the liquid (viscosity of PEG), and the PEG/C interface (contact angle), have to be introduced into Equation 1. The results for the permeability derived from Equation 1 are reported in Table IV and plotted against the square of the particle diameter in Fig. 6. The data nicely follow the empirical law according to which the permeability k of a porous medium is proportional to the square of the mean particulate diameter [10],

$$k = aD^2 \tag{3}$$

where a is a constant. The results for the compact permeability derived from the experimental results for C/A1 and those results reported in [9] for infiltration in the Al/SiC system are given in Fig. 6 and Table IV. Again, both closely follow the empirical D^2 law of Equation 3. In deriving k for C/A1, we took the viscosity given in Ref. [12] for alloy Al-12Si, approximately 0.80 mPa s. Permeability data for carbon compacts derived from A1 infiltration are significantly lower than those obtained with PEG. This can be hardly understood if one notes that, as PEG infiltration occurs under fully wetting conditions, the derived permeability should be similar to the actual intrinsic permeability of the compact (the one derived from fully saturated infiltration experiments).

TABLE IV Slope of the straight lines fitted to the experimental data for intrinsic permeability versus square of the particle diameter

			Fit	
	D (μm)	$k(\times 10^{-14})$ m^2	Slope	R^2
C/PEG	13.5	1.84	0.0074	0.99
	26	6.4		
	61.6	27.61		
C/Al-12Si	13.5	1.42	0.0028	0.98
	26	2.20		
	61.6	10.45		
SiC/Al	13	1.96	0.0055	0.96
	26	5.15		
	50	13.93		

The units of the slope are: m^2/Pa in the first case and m^2/s in the second. The regression coefficient is also given. The permeability of the compact k was derived from the slope as discussed in the text.

4. Conclusion

Experimental results for pressure infiltration of aluminium and Al-Si alloys into compacts of graphite particulate have been presented and discussed. Infiltration was carried out at not excessively high temperatures (913 K) to avoid graphite gasification. Extensive reaction between graphite and pure aluminium to produce aluminium carbide led to unreliable infiltration results. Instead, many of the data obtained for Al-Si alloys obeyed the laws which are expected to rule infiltration of liquids into porous media. In particular the results for the square of the infiltrated height is proportional to the pressure drop, as predicted by Darcy law. The threshold pressure for infiltration is shown to vary as the inverse of the particle diameter, in agreement with capillary law. However, the change in the infiltration rate as the temperature is raised is stronger than expected from the temperature dependence of the viscosity of Al-12Si alloy. The permeability of the carbon compacts derived from infiltration either of an organic fluid or the Al-12Si alloy varied as the square of the particle diameter, in agreement with a widely accepted empirical law.

Acknowledgements

This work was partially supported by Spanish MCYT (grant MAT2001-0529) and the European Community project (grant GRD 2-2001-50048). S.A. Sánchez is grateful to the Spanish Ministerio de Educación y Cultura for a predoctoral grant.

References

1. D. J. LLOYD, "Advanced Structural Materials" (Pergamon Press, New York, 1989) p. 1.
2. T. S. SRIVATSAN, I. A. IBRAHIM, F. A. MOHAMED and E. J. LAVERNIA, *J. Mater. Sci.* **26** (1991) 5965.
3. J. NARCISO, in Carbon'03, edited by A. Linares and D. Cazorla (Electronic support, Oviedo, 2003).
4. S. SCHAMM, R. FEDOU, J. P. ROCHER, J. M. QUENISSET and R. NASLAIN, *Metall. Trans. A* **22A** (1991) 2133.
5. F. DELANNAY, L. FROYEN and A. DERUYTTERE, *J. Mater. Sci.* **22** (1987) 1.
6. K. LANDRY, S. KALOGEROPOULOU and N. EUSTATHOPOULOS, *Mater. Sci. Eng.* **A254** (1998) 99.
7. A. ALONSO, A. PAMIES, J. NARCISO, C. GARCÍA-CORDOVILLA and E. LOUIS, *Metall Trans.* **24A** (1993) 1423.
8. C. GARCÍA-CORDOVILLA, E. LOUIS and J. NARCISO, *Acta Mater.* **47** (1999) 4461.
9. R. ARPÓN, J. M. MOLINA, R. A. SARAVANAN, C. GARCÍA-CORDOVILLA, E. LOUIS and J. NARCISO, *Acta Mater.* **50** (2002) 247.
10. J. BEAR, "Dynamics of Fluids in Porous Media" (Dover Publications, New York, NY, 1988).
11. N. SOBCZAK, Z. GORNY, M. KSIAZEK, W. RADZIWILL and P. ROHATGI, *Mat. Sci. Forum* **217–222** (1996) 153.
12. W. R. D. JONES and W. L. BARTLETT, *J. Instit, Metals* **81** (1952) 145.
13. G. LANG, *Aluminium* **49** (1973) 231.
14. J. GOICOECHEA, C. GARCÍA-CORDOVILLA, E. LOUIS and A. PAMIES, *J. Mater. Sci.* **27** (1992) 5247.
15. S. S. SÁNCHEZ, A. RODRÍGUEZ, J. M. MOLINA, J. NARCISO, E. LOUIS and F. RODRÍGUEZ-REINOSO (To be published).

Received 31 March
and accepted 20 October 2004